Faculty of Medical and Health Sciences, University of Poonch Rawalakot
Journal of Pharma and Biomedics
ISSN: 3007-1984(online), 3007-1976 (Print)
https://www.jpbsci.com/index.php/jpbs

Kinetics and Reusability of GG@AG-FE Nanocomposites for Sustainable Water Treatment

Noor Zaman[1], Farah Naz Talpur[1], Aamana Baloch[1], Naseem Khatoon Bhatti[3], Jameel Ahmed Baig[1], Abdul Raheem Shar[2]*, Farzana Mangrio[4], Hassan Imran Afridi[1], Rehana Keerio[4], Fida Hussain Shar[5]

[1] National Center of Excellence in Analytical Chemistry, University of Sindh Jamshoro, 76080, Pakistan.
[2] Assistant Professor of Chemistry, Govt. Degree College Thari Mirwah, Pakistan.
[3] Associate Professor of Chemistry, Govt. Girls Degree College Gambat, Pakistan.
[4] Institute of Chemistry, Shah Abdul Latif University Khairpur, Pakistan.
[5] Department of Mathematics, Shah Abdul Latif University Khairpur, Pakistan.

Received: December 29, 2025; Revised: March 27, 2026; Accepted: March 31, 2026

A B S T R A C T

The study was carried out for synthesis of guargum silver iron nanocomposite (GG@Ag-Fe) material by co-precipitation method from guargum polymer GG@ polymer for removal of nitrate pollution in drinking water. The synthesizes material was characterized by using energy dispersive X-ray analysis (EDX), fourier-transform infrared spectroscopy (FTIR) and scanning electron microscopy (SEM) analysis and ultra violet (UV) spectroscopic analysis.The GG@Ag-Fe nanocomposite was proved to be good adsorbent for removal of nitrate pollution from drinking water.Thus Response Surface Methodology (RSM) four key parameters: dose of the nanocomposite, contact time, pH, and initial nitrate concentration was evaluated for obtaining maximum nitrate degradation was used. The optimal values were achieved for maximum nitrate removal at nanocomposite dose of 1.0 mg/L, a contact time of 10.0 minutes, a pH of 6.0, and an initial nitrate concentration of 60.00 mg/L. Under these conditions, the model predicted a nitrate degradation efficiency of approximately 99.00%, while there was a good degree of match with the quadratic model with an R^2 of 0.94, best explained the experimental data. Although the proposed GG@Ag-Fe nanocomposite was produced good results for removal of nitrate pollution from real samples having concentration of 59.5 to 150.4 mg/L by 95 to 96.5%. Moreover the removal of nitrate follows first order kinetics while the reusability of GG@Ag-Fe nanocomposite 75%was achieved.

Keywords: Nitrate pollution, Response Surface Methodology, Groundwater.

Corresponding Author: *Abdul Raheem Shar*
Email: araheem.shar@salu.edu.pk

INTRODUCTION

Nitrate pollution in groundwater sources remains a significant threat to both environment as well as public health. Thus exceed from the permissible limit of 10 mg/L, it can lead to severe health issues such as methemoglobinemia ("blue baby syndrome") and nitrosamines carcinogenic (Chiu et al., 2007).The main source of nitrate pollution consist of manufacturing effluents, agricultural runoff from fertilizers and animal manure, as well as leachate from septic systems (Jin et al., 2012). In response to these challenges, researchers have actively explored and developed various nitrate removal technologies, including ion exchange (Ghafari, et al., 2008), biological denitrification (Eneji et al., 2013), electrodialysis (Rautenbach, 1986), chemical reduction (Wang, et a., 2014), reverse osmosis (Shrimali et al., 2001) and adsorption (Öztürk et al., 2004). However, many of these conventional methods face limitations such as high operational costs, low

efficiency, complex operation, and the potential generation of secondary pollutants (Katheresan et al., 2018).

Among these approaches, Adsorption is thought to be the most beneficialtechniques because of its simplicity, cost-effectiveness, energy efficiency, environmental compatibility, with high removal efficiency (Qasem et al., 2021). Besides the combination of adsorption along photocatalytic degradation has improved the degradation capacity of both natural as well as synthetic contaminants (Zaman et al., 2020). For improved adsorption production , scientist have concentrating on developing adsorbents having large surface areas and different functionalities includes zeolites (Maharana & Sen, 2021), carbon nano tubes (Sajid et al., 2022), metal-organic frameworks (Adegoke et al., 2020), and activated carbons (Ferreira & De Melo, 2021) have been analyzed (Mignon, et al., 2019; Ding et al., 2022; Jalili et al., 2024; Mandal et al., 2023). Polysaccharides can be used as better adsorbent capacities because these are composed of reactive functional groups which are responsible for easy chemical alteration (Wei et al., 2017).

However the ability of polysaccharides to form nanocomposite with various functional materials opens directions for developing new adsorbents with high-ranking performance (Saya et al., 2021). To obtain the better adsorption results the GG@Ag-Fe nanocomposite have been synthesized for removal of nitrate pollution from drinking water.This study refers the fabrication of ecofriendly GG@Ag-Fe absorbent for efficient removal of nitrate pollutant from drinking water". The results indicate the potential of GG@Ag-Fe nanocomposite for removal of nitrate pollutant in drinking water was superior as eco-friendly, creating new ways for future research and development in water purification technologies.

MATERIALS AND METHODS

Reagents and apparatus

Guar gum was purchased from local vendor while silver nitrate andiron (II) sulfate were purchased from Sigma–Aldrich. A REX-C410 model hot plate was used for heating while for separation and purification processes aCenturion centrifuge was used. More equipmentorbital shaker for uniform mixing, an electronic digital balance for precise mass measurements and a micropipette was employed for accurate volumetric calibration and handling of small volumes of reagents was used also.The water used in this workwas distilled and deionized.

Synthesis of GG@Ag-Fe nanocomposite

The 1.7 g of silver nitrate and 1.52 g of iron(II) sulfate were each dissolved in 100 mL of distilled water, yielding 0.1 M solutions. The guar gum solution was mixed with the prepared 0.1M silver nitrate and 0.1 M iron (II) sulfate solutions in a volumetric ratio of 1:1:4, respectively to synthesized the eco-friendly, non-toxic, and economically viable approach, as schematically shown in Figure 1.The reaction mixture was maintained at 90 °C on a hotplate for 15 minutes. A noticeable reddish-brown color wasdeveloped during heating, confirms the formation of GG@Ag-Fe nanocomposite. After heating, the mixture was left to cool naturally to room temperature. The resulting product was thoroughly rinsed with distilled water to eliminate any unreacted substances. The washed synthesized GG@Ag-Fe nanocomposite was dried in an oven, and stored in airtight containers for characterization to confirm successful synthesis.

Characterization techniques

The GG@Ag-Fe nanocomposite was characterized by scanning electron microscopy and energy dispersive x-ray analysis for used for confirmation of surface morphology and structure while of required the elemental composition (SEM, EDX Hitachi S4300). The IR spectra were obtained with a Bio-Rad FTS 3000 spectrometer from Digilab (Cambridge, USA) with KBr beam splitter, detector at 8 cm−1resolution and 300scans per sample while ultraviolet–visible (UV–vis) spectra in the range 200–800 nm were obtained with a diode array spectrophotometer (HP 8452A, Hewlett Packard, Waldbronn, Germany) for the identification of required functional groups, chemical bonds and optical properties (Bashir et al., 2024).

Nitrate removal

The synthesized GG@Ag-Fe nanocomposite was used to remove the nitrate pollutants in drinking water with varying experimental conditions. Aqueous sodium nitrate solutions was used to prepare the standard solution of nitrate 20 to 100 mg/L across a pH spectrum of 2 to 10 with dosage of the nanocomposite between 0.5 and 1.5 mg/L, contact time in the range of 5 to 15 minutes was optimized . The nanocomposite solution was well mixed in a glass beaker at room temperature was sonicated for 1 minute, which formed a stable suspension. After 15minute, the nanocomposite was separated via centrifugation. The supernatant was then analyzed for residual nitrate concentration using a DR/2800 colorimeter, as described by (Nabid et al., 2013). The RSM was used toidentify the optimal parameter combination to attain either the maximum response values from, both the individual and combined effects of four critical parameters like as: A**:** dose of composite (mg/L), B: time (min), C: pH and D: nitrate (mg/L), on nitrate removal (%). A User-Defined Design (UDD) three-level, coded as -1, 0, and 1

corresponded to the low, medium, and high values of each factor are listed in the accompanying table 1.

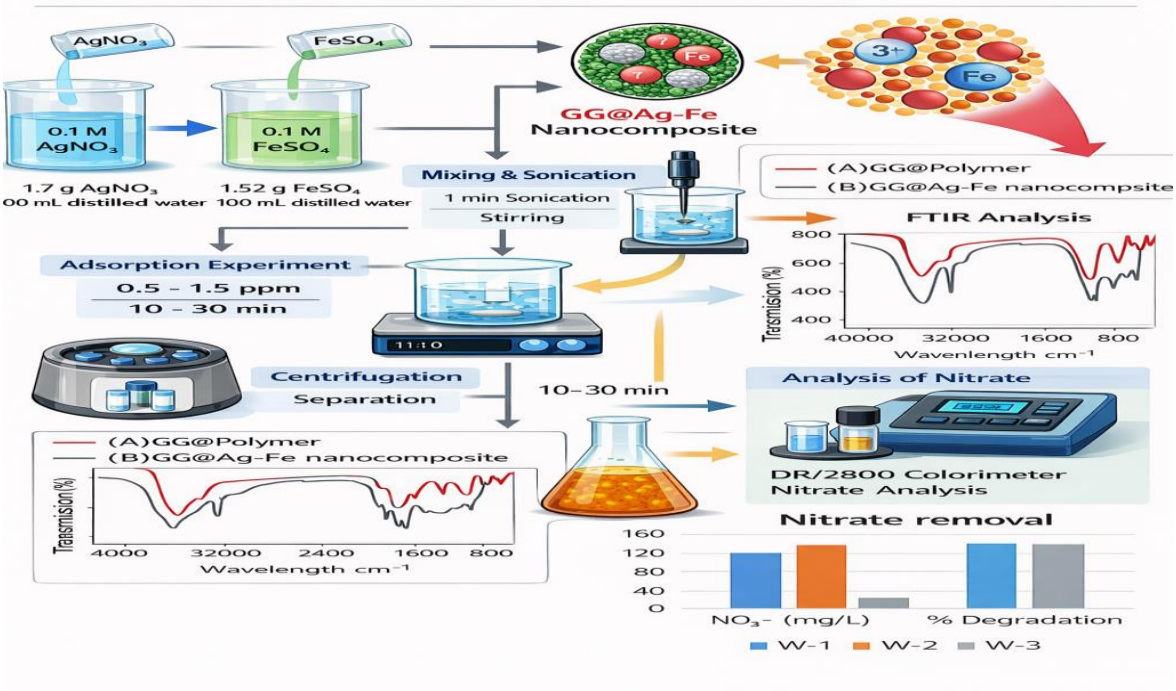

Figure 1: Systematic diagram of synthesis of GG@Ag-Fe Nanocomposite for removal of nitrate pollution.

Table 1: Parameter and their levels (UDD).

Variables	Unit	Symbol	Levels		
			Low	Intermediate	Higher
			Level (-1)	Level (0)	Level (+1)
Dose of composite	mg/L	A	0.5	1	1.5
Time	min:	B	5	10	15
pH	$[H^+]$	C	2	6	10
Nitrate	mg/L	D	20	60	100

RESULTS AND DISCUSSION

UV-Visible Spectrophotometry

The UV–Visible absorption spectra of GG@polymer and GG@Ag-Fe nanocomposite are shown in figure 2. (a and b). In Fig.2 (a) the GG@polymer displays a strong and sharp absorbance peak around 220–250 nm, which can be attributed to π→π* or n→π* electronic transitions of chromophoric groups present in the polymer matrix. In Figure 2 (b), the GG@Ag-Fe nanocomposite shows slightly lower absorbance intensity with a broader and red-shifted peak indicates successful incorporation of Ag and Fe nanoparticles into the polymer framework. Furthermore, the nanocomposite exhibits extended absorbance into 300–600 nm, which can be ascribed of successful incorporation silver-iron nanoparticles confirm the formation of a metal–polymer nanocomposite.

FTIR analysis

FT-IR spectroscopy was employed to identify the functional groups present in GG@polymer and the synthesized GG@Ag-Fe nanocomposite, as illustrated in Figure 3 (a and b) the Figure: 3(a) shows the spectrum of GG@polymerat 3424, 3021, 1654, 1447, and 1027 cm^{-1} shows the O–H stretching due to hydrogen bonding in polysaccharides, C–H stretching of alkanes, C=O stretching of carbonyl or ester groups, C–H bending of CH_2 groups, and C–O–C and C–O stretching vibrations of the polysaccharide backbone, respectively.The Figure 3 (b)shows the spectrum GG@Ag-Fenanocomposite at 3428 cm^{-1} indicates O–H stretching vibrations of hydroxyl groups. Additional peaks at 3003, 1640, 1424, and 1030 cm^{-1} are attributed to C–H stretching, C=O stretching, C–H bending, and C–O–C/C–O stretching

of the polysaccharide structure. Compared to GG@polymer, these bands show slight shifts: for example, the peaks at 3021, 1640, 1427, and 1027 cm^{-1} in GG@polymer shifted to 3003, 1654, 1424, and 1030 cm^{-1} in the GG@Ag-Fe Nanocomposite as shown in figure 2.0 (b). These spectral shifts, particularly the increase in O–H stretching frequency and the downward shifts in other functional groups, suggest strong interactions between the hydroxyl groups of GG@polymer and the Ag and Fe ions in the GG@Ag-Fe nanocomposite matrix, confirming successful incorporation and coordination of the metal ions within the polymeric network (Khan et al., 2020).

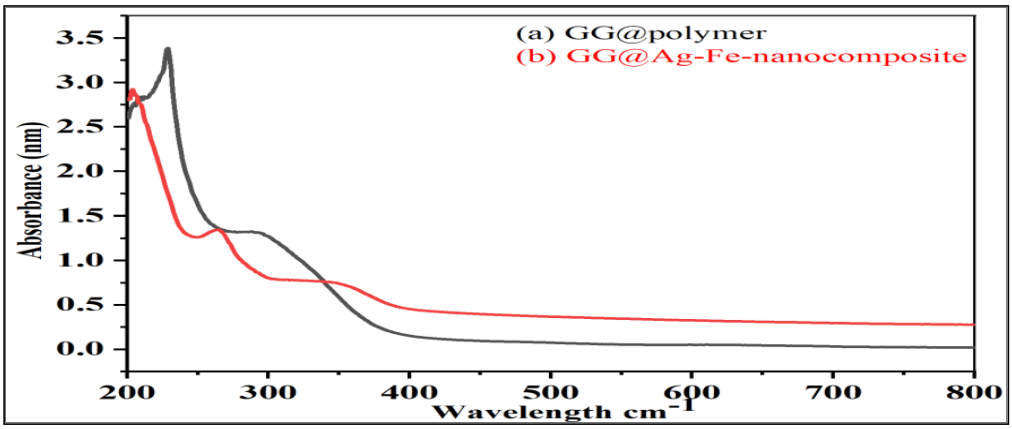

Figure 2: UV analysis of (a) GG@polymer (b) GG@Ag-Fe.

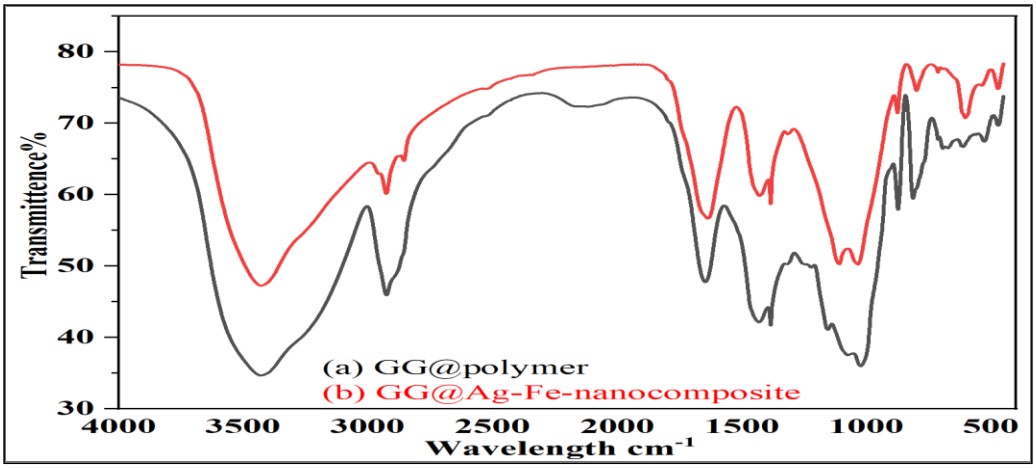

Figure 3: FTIR analysis of (a) GG@polymer (b) GG@Ag-Fe.

SEM Analysis

The surface morphology, structural features, and internal architecture of the GG@polymer and GG@Ag-Fe nanocomposite were examined using scanning electron microscopy (SEM), as depicted in Figure 4 (a and b). The SEM image of GG@polymer shows the polygonal non-regular shape shown in Figure 4(a). The SEM micrographs of GG@Ag-Fe nanocomposite reveal a leaf-like morphology with irregularly shaped domains which are homogeneously distributed, indicative of silver–iron nanoparticles embedded within the guar gum matrix as shown in Figure 4(b). The images suggest a homogeneous distribution of Ag-Fe nanoparticles (AgFeNPs) throughout the polymeric network. The particle size analysis based on SEM observations indicates that the AgFeNPs possess diameters in the range of approximately 50nm, with uniform dispersion across the nanocomposite surface.

EDX Analysis

The EDX spectrum of theGG@polymer and GG@Ag-Fe nanocomposite shown in Figure 5(a and b). The Figure 5(a) shows the carbon oxygen as main elements in GG@polymer while the Figure 5(b) confirms the presence of carbon, oxygen, platinum, and silver elements, verifying the successful synthesis of the GG@Ag-Fe nanocomposite.

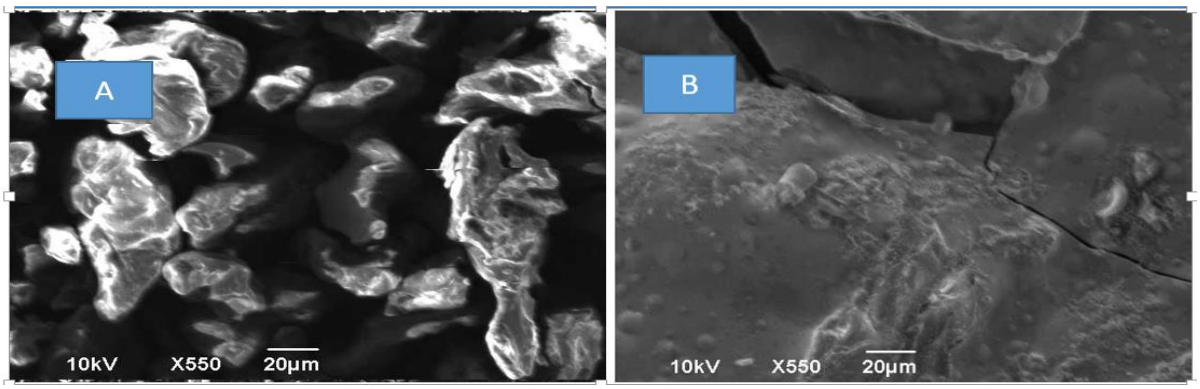

Figure 4: SEM analysis of (a) GG@Polymer (b) GG@Ag-Fe.

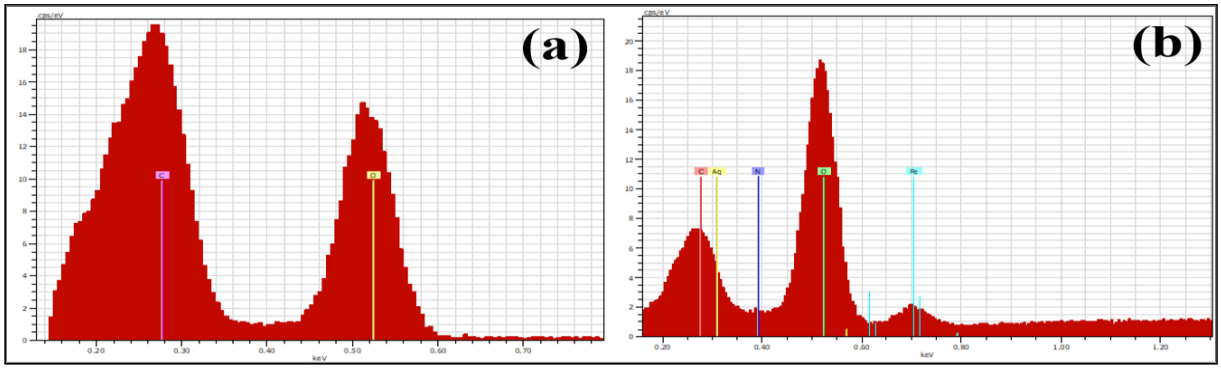

Figure 5: EDX analysis of (a) GG@Polymer (b) GG@Ag-Fe.

Effect of GG@Ag-Fenanocomposite Removal of Nitrate Pollutant From drinking Water

A detail experimental process was carried out at various ranges of variable as shown in table 2. The table 2 shows the experimental variables for nitrate removal .To evaluate the effect of varying GG@Ag-Fenanocomposite concentrations on nitrate removal, the different nanocomposite ratios were investigated which shows different removal efficiency as given in bellow table 2. The nanocomposite, nitrate, pH and time exhibited optimal removal efficiency at a concentration of 1.0, 60 mg/L, 6 and 10 minutes respectively. For the purpose of optimizing other operational parameters, a concentration nanocomposite was 1.mg/L was selected, owing to its superior physical stability during repeated use. At concentrations higher than 1.0 mg/L, a noticeable decline in structural integrity and dispersion stability was observed. The enhanced ion-exchange capacity of natural polymers, attributed to the presence of exchangeable counter-ions, rendered them more effective in nitrate adsorption compared to synthetic polymers.

The, GG@polymer demonstrated superior performance, likely due to increased electron mobility along its molecular backbone, which facilitates ion-exchange interactions. The adsorption efficacy of the GG@Ag-Fe nanocomposite was further evaluated under varying pH conditions, temperatures, and in the presence of different dopants, confirming its robustness and versatility as an efficient nitrate adsorbent. One of the key advantages of the GG@Ag-Fe nanocomposite is its ease of in situ synthesis through a green chemical route, utilizing acidic GG@polymerand silver–iron salts in the presence of mild oxidizing agents.

Table 2: Experimental variables for Nitrate removal.

Run	Factor 1	Factor 2	Factor 3	Factor 4	Response 1
	A: Nitrate Concentration	B: Amont of Nanocomposite	C: Time	D: pH	Nitrate removal
	mg/L	mg/L	Minutes	-	%
1.	20	0.5	5	10	13
2.	100	0.5	15	10	78

3.	100	1.5	5	10	93
4.	20	0.5	15	10	33
5.	100	1.5	15	10	98
6.	60	1	10	2	79
7.	100	0.5	5	2	98
8.	60	1	10	6	86
9.	60	1	10	6	99
10.	20	1	10	6	55
11.	20	0.5	15	2	22
12.	100	0.5	15	2	84
13.	100	1.5	15	2	80
14.	60	1	10	6	85
15.	20	0.5	5	2	45
16.	60	1	10	10	22
17.	20	1.5	15	2	86
18.	20	1.5	5	2	94
19.	20	1.0	10	6	85
20.	100	1.5	5	2	94
21.	100	0.5	5	10	71
22.	20	1.5	15	10	82
23.	60	1	10	6	44
24.	60	1	10	6	82
25.	20	1.5	5	10	43
26.	60	1.0	10	6	70
27.	100	1	10	6	94

ANOVA for Cubic Model and Regression Model Description

A regression model was developed to predict nitrate degradation based on four key variables: A, B, C, and D and its positive and negative AB, AC, AD, BC, BD, and CD shows increase and decreased degradation while the enhance model reliability and predictive capability are also as given in Table 3. The Regression model in table 4.0 confirms second-order quadratic polynomial between the response and the independent variables such as A, B, C, and D. The intercept value 84.93 represents the predicted response at the coded zero levels of all factors and individual influence of each variable on the response, where positive coefficients for A, B, and C demonstrate a synergistic effect, while the negative coefficient of D reflects an antagonistic influence.

The interaction terms AB, AC, AD, BC, BD, and CD) explain the combined effect of two variables on the response, indicating that the influence of one factor is dependent on the level of another, while A^2, B^2, C^2, and D^2 confirms the non-linear behavior of the system and the existence of curvature in the response surface, which is essential for process optimization. The $R^2 = 0.9407$, indicating that 94.07% of the variability in the response is explained by the regression equation while the adjusted R^2 value 0.8716 further validates the statistical reliability of the model terms and excluding insignificant contributions. The close values of R^2 and adjusted R^2 confirms model is fit and suitable for prediction and optimization within the studied experimental range.

Table 3: ANOVA for Quadratic model for nitrate degradation.

Source	Sum of Squares	df	Mean Square	F-value	p-value	S/N-Sig
Model	17994.85	14	1285.35	13.60	< 0.0001	significant
A-Nitrate Concentration	5582.72	1	5582.72	59.08	< 0.0001	
B-Amont of Nanocomposite	3192.25	1	3192.25	33.78	< 0.0001	
C-Time	9.00	1	9.00	0.0952	0.7629	
D-pH	662.37	1	662.37	7.01	0.0213	
AB	1560.25	1	1560.25	16.51	0.0016	
AC	121.00	1	121.00	1.28	0.2799	

AD	225.00	1	225.00	2.38	0.1488
BC	64.00	1	64.00	0.6773	0.4266
BD	16.00	1	16.00	0.1693	0.6880
CD	1056.25	1	1056.25	11.18	0.0059
A^2	166.30	1	166.30	1.76	0.2093
B^2	593.05	1	593.05	6.28	0.0276
C^2	1281.93	1	1281.93	13.57	0.0031
D^2	2857.95	1	2857.95	30.25	0.0001

Table 4: Regression model equation for response against the different factors and their interaction.

Model Equation	R^2	Adjusted R^2
+84.93 +17.61 A+14.13B+0.7500C-6.08D-9.88AB-2.7AC+3.75AD+2.00 BC+1.0000BD+8.12 CD-10.43A^2+21.21B^2-10.61C^2-15.48D^2	0.9407	0.8716

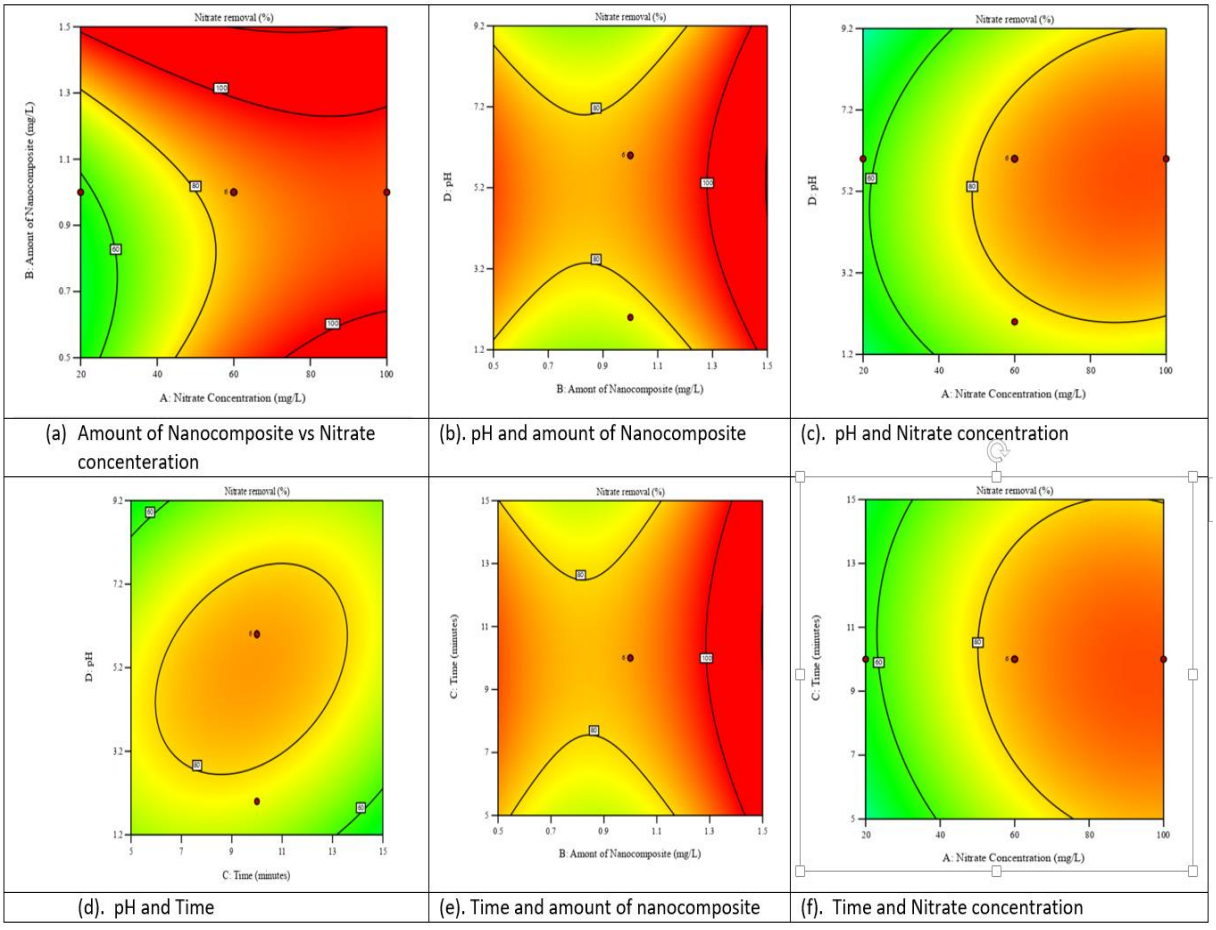

Figure 6: Contour plot of interaction effects (a) Amount of Nanocomposite vs Nitrate concentration (b) pH and amount of Nanocomposite (c) pH and Nitrate concentration (d) pH and Time (e) Time and amount of nanocomposite (f) Time and Nitrate concentration for nitrate degradation using GG@Ag-Fe Nanocomposite.

Optimization of Parameter

Figure 7 shows the optimization ramp. The optimization graph illustrates the ideal conditions for achieving maximum nitrate degradation using RSM. Four key parameters were evaluated: dose of the nanocomposite, contact time, pH, and initial nitrate concentration. The

optimal values determined were a nanocomposite dose of 1.0mg/L, a contact time of 10.0 minutes, a pH of 6.0, and an initial nitrate concentration of 60.0 mg/L predicted a nitrate of approximately 99.0%. The desirability score of 1.000 indicates that these parameter values represent the most favorable combination within the tested range, ensuring maximum response output. This optimized solution, ranked 1 out of 100, confirms the effectiveness of the selected conditions in enhancing nitrate removal from aqueous solutions.

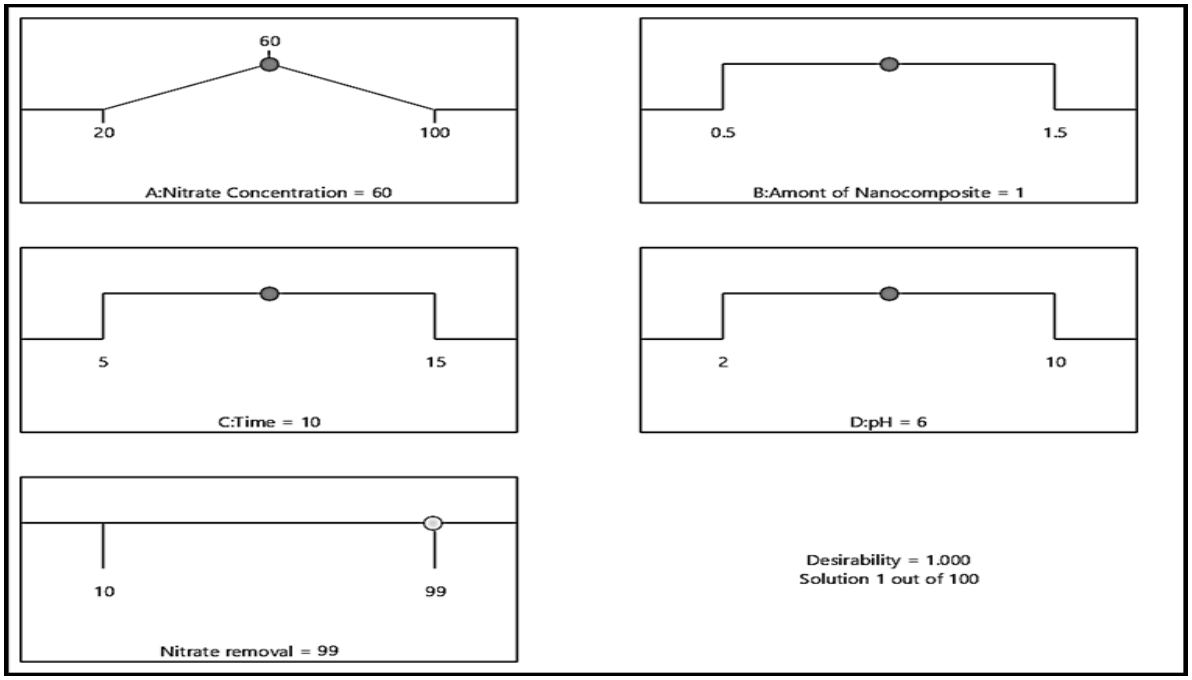

Figure 7: Optimization ramp.

Response Contour Plots

Figure 6 illustrates the 2D contour plots derived from RSM, depicting the interactive effects of key process variables on nitrate degradation efficiency. The plot (a) shows the combined influence of amount of nanocomposite vs nitrate concentration a significant enhancement in nitrate removal was observed with increasing both parameters the amount of nanocomposite as well as nitrate concentration at 1.4 and 60 mg/L, respectively, reaching an optimum around approximately 100.0%. Thus plot (b) demonstrates interactive effects of pH and amount of nanocomposite for maximum nitrate removal efficiency approximately 100.0 % when pH is reaches 5.2 and amount of nanocomposite at 1.4 mg/L, highlighting pH sensitivity. Plot (c) reveals the interaction between pH and nitrate concentration where a nitrate dose and pH reaches at ~60 mg/L and 6.0 respectively nitrate removes 100.0 %. The plot (d) shows the interaction of pH and time result in enhanced removal around 100.0% when the pH and time is 6.0 , is 10.0 respectively while further increase in either parameter reduces efficiency. The plot (e) shows interaction of time and amount of nanocomposite, while at 10.0 minutes , 1.0 mg/L observed maximum removal of approximately 100.0%. Lastly, plot (f) demonstrate the time and nitrate concentration nitrate removal efficiency, which shows approximately 80.0% removal under 10.0 minutes s and lightly nitrate concentration of 60.0 mg/L. Overall, the plots confirm that optimal nitrate degradation (99.0) occurs at composite dose 1.00 mg/L, contact time 10.0 min, pH 6.00, and nitrate concentration 60.0mg/L.

Performance evaluation by RSM

Figure 8 showsthe actualvs predicted value for degradation of nitrate from ground water, which is strong agreement between the model's predicted values and the actual observed values. Each data point represents a specific observation, with its actual value plotted on the x-axis and the predicted value on the y-axis. The majority of points are closely clustered around the diagonal 45-degree line, which represents perfect prediction and high accuracy and consistency across the entire range of values. The color gradient and numbered labels suggest the data points may belong to different categories or ranges, but regardless of

these groupings, the model appears to maintain reliable performance without significant deviation. Overall, the plot confirms that the model has a strong predictive capability, making it a good fit for the data.

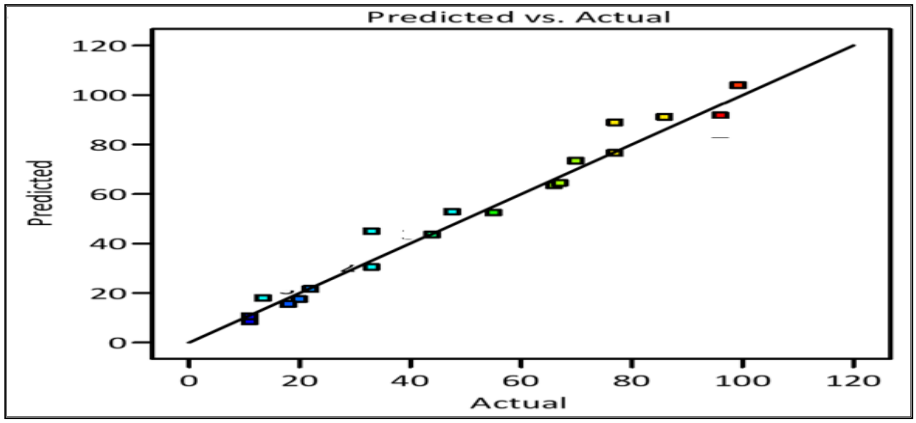

Figure 8: Actual vs. predicted value.

Kinetic Research on Nitrate Removal

The kinetics of nitrate removal was assessed by using the pseudo-first-and pseudo- second-order models are shown in Figure 8 (a and b). Obtained outcomes of rate constant for theoretical and calculated values match for first-order model where values of theoretical and calculated measured was 1.91 and 1.81 mg/g respectively, while for pseudo-second - order model don't confirm measured value for theoretical and calculated was found 1.91 was 4.26 respectively.

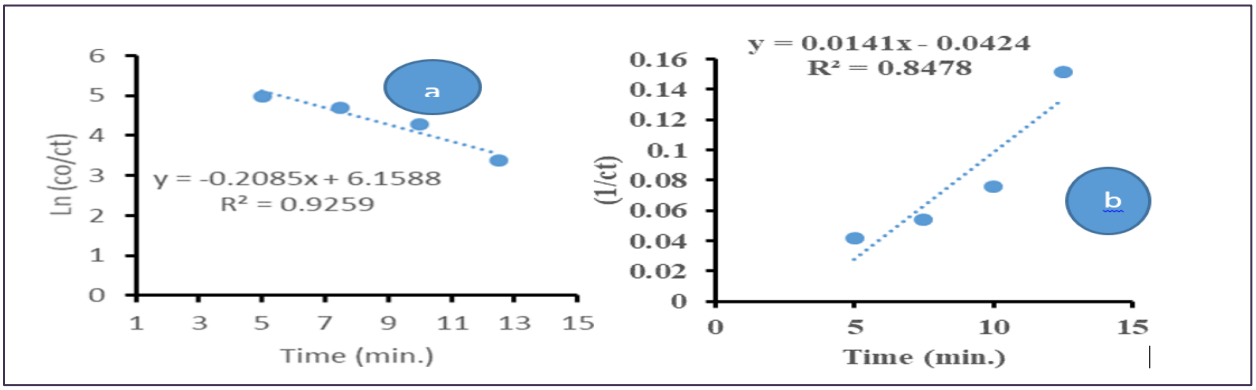

Figure 9: (a) Pseudo= First order (b) Pseudo second order model.

Mechanism of Removal of Nitrate from Water by GG@Ag-Fe-Nanocomposite

The removal of nitrate follows physicochemical adsorption and sequestration processes .The guar gum provides hydroxyl groups which interact through electrostatically with nitrate anions. Iron reduces the nitrate into nitrogen gas .Silver nanoparticles enhance the accessible surface area and electrostatic heterogeneity of the composite. Collectively, nitrate removal occurs by (i) rapid outer-sphere electrostatic attraction to positively charged/ protonated surface sites at the polymer–metal interface (ii) slower inner-sphere adsorption via ligand exchange onto Fe–OH moieties and/or complexation with functional groups of guar gum, and (iii) physical entrapment or pore-filling of nitrate within the hydrated polymeric network (Riaz & Ashraf, 2015). The net result is sequestration of NO_3^-as surface-bound species and within the composite matrix; desorption is controlled by ionic strength and pH indicating predominance of electrostatic and surface- complexation interactions rather than irreversible transformation.

Electrostatic adsorption (outer-sphere)

$S\text{-}H^+ + NO_3^- \rightleftarrows S\text{-}H^+ \cdot NO_3^-$

Ligand exchange / inner-sphere complexation on iron oxyhydroxide sites

$\equiv Fe\text{-}OH + NO_3^- \rightleftarrows \equiv Fe\text{-}NO_3^- + OH$

Ion-exchange type interaction with polymer functional

sites

$R\text{-}OH + NO_3^- \rightleftarrows R\text{-}NO_3^- + OH$

Physical entrapment / pore filling (qualitative)

$NO_{3\,(aq)}^- \rightarrow NO_{3\,\text{polymer pores}}^-$

Application of nitrate removal samples fromreal samples

The experimental results for nitrate removal are summarized in Table 5 highlight the nitrate (NO_3^-) removal efficiency achieved by GG@Ag-Fe-nanocomposite in real sample analysis also. Three different well water samples (W-1, W-2, and W-3) collected from Mitti, Tharpar desert for real sample analysis shows greatest nitrate removal even at more than 150 ppm level.

Table 5: Nitrate removal samples from real samples.

	NO_3^-	After treatment with GG@Ag-Fe	Degradation
SAMPLE	mg/L	mg/L	%
W-1	59.5	1.26	96.5
W-2	135.3	4.05	96.0
W-3	150.4	7.52	95.0

Reusability of GG@Ag-Fe – nanocomposite

Figure 10.0 shows the reusability of GG@Ag-Fe nanocomposite for nitrate removal from water and waste water. Five consecutive nitrate removal tests were performed in triplicate at optimal conditions (1.0 mg/L of catalyst, pH of 6.0, of 10 min, 50.0mg/Nitrate) to study the reusability of the of GG@Ag-Fe catalyst. After each reaction, the adsorbent was separated by an external magnetic field to consider its reusability. According to this, the adsorption capability remained 75% after five times repeated usage. Polymer-based nanocomposites incorporating chitosan, cellulose, or guar gum matrices loaded with nanoparticles (e.g., Fe_3O_4, TiO_2, or ZnO) have also demonstrated excellent adsorption capacity and easy regeneration, combining the advantages of biopolymer stability and nanomaterial reactivity (Agorku et al., 2023).

Comparison of current research with other studies

The comparison of current research with other study is given below Table 6. A variety of composite systems have been investigated for the removal of nitrate from aqueous solutions, and their performances vary depending on the synthesis method, operating conditions, and material characteristics. However the experimental data listed below shows the performance GG@Ag-Fenanocomposite is supreme to all material synthesized.

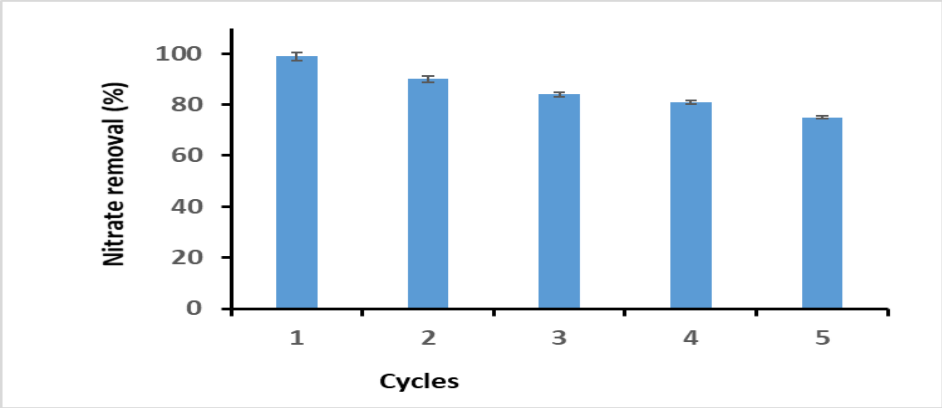

Figure 10: Resuability of GG@Ag-.

Table 6: Comparison of current research with other studies.

Composite System	pH	Time	Composite	Nitrate Removal	Reference
Unit	-	(Mint)	(g/L)	(%)	-
Multi-walled carbon nanotubes (MWCNTs) with (PANI), polypyrrole (PPY), poly(1,8-diaminonaphthalene) [P(1,8- DAN)] and poly(2-					(Nabid, et al.,2013)

vinylpyridine) (P2VP	6.5	0.0	1.00	80.00	
Bimetal oxide Alumina and Iron(III)OxideasNylon6, 6 and Poly (sodium-4- styrenesulphonate) as polymer matrix	7.0	0.0	100.0	34.78	(Saxena and Saxena, 2016)
Development and Application of GrapheneOxide/Poly-AmidoaminesDendrimers(GO/PAMAMs) Nano-Composite for Nitrate Removal from Aqueous Solutions	7.5	15	0.025	90.00	(Alighardashi, et al., 2018)
New magnetic Co3O4/Fe3O4 doped polyaniline nanocomposite for the effective and rapid removal of nitrate ions from ground water samples	6.0	60.0	0.06	68.96	(Esmaeili Bidhendi, et al., 2020)
Green Synthesis of GG@Ag-FeNanocomposite for Effective Nitrate Removal from Drinking Water	6.0	10.0	0.001	99.00	Current Study

CONCLUSION

In this study, a GG@Ag–Fe nanocomposite was successfully synthesized using natural guar gum as a polymer matrix and silver–iron metal nanoparticles via a co-precipitation method for the efficient removal of nitrate from drinking water. Optimization through Response Surface Methodology (RSM) demonstrated a maximum nitrate degradation efficiency of 99.0% at pH 6.0 within 10 minutes, using a nanocomposite dose of 1.0 mg L^{-1} and an initial nitrate concentration of 60 ppm. The nitrate degradation process followed pseudo-first-order kinetics, indicating favorable reaction behavior. Reusability studies revealed that the nanocomposite retained 75.0% of its degradation efficiency after repeated use. Furthermore, the applicability of the GG@Ag–Fe nanocomposite was validated using real water samples collected from Mithi, Tharparkar, and achieving 96.5% nitrate removal at a higher nitrate concentration of 150 mg L^{-1}. These results confirm the GG@Ag–Fe nanocomposite as an effective, rapid, and sustainable material for nitrate remediation in drinking water systems.

AUTHOR'S CONTRIBUTION

Noor Zaman and Hassan Imran Afridi conceptualized the study, synthesized the materials, designed the experiments, and Aamana Baloch was responsible for data collection and analysis. Jameel Ahmed Baig and Naseem Khatoon Bhatti conducted the material characterizations. Fida Hussain Shar and Farzana Mangrio assisted in characterizations and contributed to the interpretation of the results and Response Surface Methodology (RSM) analysis. Abdul Raheem Shar and Rehana Keerio formatted the manuscript and edited the initial draft. Farah Naz supervised the entire project and critically reviewed the manuscript. All authors read, revised, and approved the final version of the manuscript.

ACKNOWLEDGEMENTS

The authors acknowledge the facilities provided by National Center of Excellence University of Sindh, Jamashoro and also technical support provided by process simulation and modeling research group, Department of Chemical Engineering Mehran University of Engineering and Technology Jamshoro.

REFERENCES

Adegoke, K.A., Agboola, O.S., Ogunmodede, J., Araoye, A.O. and Bello, O.S. (2020) 'Metal–organic frameworks as adsorbents for sequestering organic pollutants from wastewater', *Materials Chemistry and Physics*, 253, 123246.

Agorku, E.S., Kangmennaa, A., Haruna, M. and Opoku, F. (2023) 'Photocatalytic activity of red-emission PVA-$GdVO_4:Eu^{3+}$ nanocomposite towards the degradation of Eosin Y in water', *Sustainable Environment*, 9(1), 2266632.

Alighardashi, A., Kashitarash Esfahani, Z., Najafi, F., Afkhami, A. and Hassani, N. (2018) 'Development and application of graphene oxide/poly(amidoamine) dendrimer (GO/PAMAM) nanocomposite for nitrate removal from aqueous solutions', *Environmental Processes*, 5(1), pp. 41–64.

Bashir, N., Gulzar, S. and Shad, S. (2024) 'Green synthesis of silver and iron nanocomposites using aqueous

extract of *Zanthoxylum armatum* seeds and their application for removal of Acid Black 234 dye', *Frontiers in Toxicology*, 6, 1288783.

Chiu, H.F., Tsai, S.S. and Yang, C.Y. (2007) 'Nitrate in drinking water and risk of death from bladder cancer: an ecological case–control study in Taiwan', *Journal of Toxicology and Environmental Health, Part A*, 70(12), pp. 1000–1004.

Eneji, A.E., Islam, R., An, P. and Amalu, U.C. (2013) 'Nitrate retention and physiological adjustment of maize to soil amendment with superabsorbent polymers', *Journal of Cleaner Production*, 52, pp. 474–480.

Esmaeili Bidhendi, M., Asadi, Z., Bozorgian, A., Shahhoseini, A., Gabris, M.A., Shahabuddin, S., Khanam, R. and Saidur, R. (2020) 'Magnetic Co_3O_4/Fe_3O_4-doped polyaniline nanocomposite for rapid removal of nitrate ions from groundwater samples', *Environmental Progress & Sustainable Energy*, 39(1), e13306.

Ferreira, L.M. and Melo, R.R. (2021) 'Use of activated charcoal as a bio-adsorbent for treatment of residual waters: a review', *Nativa*, 9, pp. 215–221.

Ge, H., Ding, K., Guo, F., Wu, X., Zhai, N. and Wang, W. (2022) 'Green and superior adsorbents derived from natural plant gums for removal of contaminants: a review', *Materials*, 16(1), 179.

Ghafari, S., Hasan, M. and Aroua, M.K. (2008) 'Bio-electrochemical removal of nitrate from water and wastewater: a review', *Bioresource Technology*, 99(10), pp. 3965–3974.

Jalili, M., Meftahizade, H., Golafshan, A., Zamani, E., Zamani, M., Behzadi Moghaddam, N. and Ghorbanpour, M. (2024) 'Green-synthesized guar plant composites for wastewater remediation: a comprehensive review', *Polymer Bulletin*, 81(1), pp. 247–273.

Jin, Z., Pan, Z., Jin, M., Li, F., Wan, Y. and Gu, B. (2012) 'Determination of nitrate contamination sources using isotopic and chemical indicators in an agricultural region in China', *Agriculture, Ecosystems & Environment*, 155, pp. 78–86.

Katheresan, V., Kansedo, J. and Lau, S.Y. (2018) 'Efficiency of various recent wastewater dye removal methods: a review', *Journal of Environmental Chemical Engineering*, 6(4), pp. 4676–4697.

Khan, N., Kumar, D. and Kumar, P. (2020) 'Silver nanoparticles embedded guar gum/gelatin nanocomposite: green synthesis, characterization and antibacterial activity', *Colloid and Interface Science Communications*, 35, 100242.

Maharana, M. and Sen, S. (2021) 'Magnetic zeolite: a green reusable adsorbent in wastewater treatment', *Materials Today: Proceedings*, 47, pp. 1490–1495.

Mandal, S., Hwang, S. and Shi, S.Q. (2023) 'Guar gum, a low-cost sustainable biopolymer for wastewater treatment: a review', *International Journal of Biological Macromolecules*, 226, pp. 368–382.

Mignon, A., De Belie, N., Dubruel, P. and Van Vlierberghe, S. (2019) 'Superabsorbent polymers: a review on the characteristics and applications of synthetic, polysaccharide-based, semi-synthetic and "smart" derivatives', *European Polymer Journal*, 117, pp. 165–178.

Nabid, M.R., Sedghi, R., Sharifi, R., Oskooie, H.A. and Heravi, M.M. (2013) 'Removal of toxic nitrate ions from drinking water using conducting polymer/MWCNT nanocomposites', *Iranian Polymer Journal*, 22(2), pp. 85–92.

Öztürk, N. and Bektaş, T.E. (2004) 'Nitrate removal from aqueous solution by adsorption onto various materials', *Journal of Hazardous Materials*, 112(1–2), pp. 155–162.

Qasem, N.A., Mohammed, R.H. and Lawal, D.U. (2021) 'Removal of heavy metal ions from wastewater: a comprehensive and critical review', *npj Clean Water*, 4(1), 36.

Rautenbach, R. (1986) 'Separation of nitrate from well water by membrane processes (reverse osmosis/electrodialysis reversal)', *Aqua*, 5, pp. 279–282.

Riaz, U. and Ashraf, S.M. (2015) 'Microwave-induced catalytic degradation of a textile dye using bentonite–poly(o-toluidine) nanohybrid', *RSC Advances*, 5(5), pp. 3276–3285.

Sajid, M., Asif, M., Baig, N., Kabeer, M., Ihsanullah, I. and Mohammad, A.W. (2022) 'Carbon nanotube-based adsorbents: properties, functionalization, interaction mechanisms and applications in water purification', *Journal of Water Process Engineering*, 47, 102815.

Saxena, S. and Saxena, U. (2016) 'Development of bimetal oxide-doped multifunctional polymer nanocomposite for water treatment', *International Nano Letters*, 6(4), pp. 223–234.

Saya, L., Malik, V., Singh, A., Singh, S., Gambhir, G., Singh, W.R., Chandra, R. and Hooda, S. (2021)

'Guar gum-based nanocomposites: role in water purification through efficient removal of dyes and metal ions', *Carbohydrate Polymers*, 261, 117851.

Shrimali, M. and Singh, K.P. (2001) 'New methods of nitrate removal from water', *Environmental Pollution*, 112(3), pp. 351–359.

Wang, T., Lin, J., Chen, Z., Megharaj, M. and Naidu, R. (2014) 'Green synthesis of iron nanoparticles using green tea and eucalyptus leaf extracts for nitrate removal in aqueous solution', *Journal of Cleaner Production*, 83, pp. 413–419.

Wei, X., Huang, T., Yang, J.H., Zhang, N., Wang, Y. and Zhou, Z.W. (2017) 'Green synthesis of hybrid graphene oxide/microcrystalline cellulose aerogels and their use as superabsorbents', *Journal of Hazardous Materials*, 335, pp. 28–38.

Zaman, A., Orasugh, J.T., Banerjee, P., Dutta, S., Ali, M.S., Das, D., Bhattacharya, A. and Chattopadhyay, D. (2020) 'Facile one-pot in situ synthesis of graphene oxide–cellulose nanocomposite for enhanced azo dye adsorption under optimized conditions', *Carbohydrate Polymers*, 246, 116661.